

# Power System Harmonic Reduction Using Shunt Active Filter

OGBOH V. C.<sup>1</sup>, EZEUDE M. G.<sup>2</sup>, ANIONOVO U. E.<sup>3</sup>, ODIGBO A. C.<sup>4</sup>, OGBOKE H. N.<sup>5</sup>

<sup>1, 2, 3, 4, 5</sup>Department of Electrical Engineering, Nnamdi Azikiwe University, Awka, Anambra State, Nigeria

**Abstract-** *The increasing penetration of power electronic converters, nonlinear loads, and distributed generation units into modern power systems has significantly heightened the problem of harmonic distortion, adversely affecting power quality and system reliability. This paper presents an investigation into power system harmonic reduction using a Shunt Active Power Filter (SAPF). The shunt active filter is designed to inject compensating currents that counteract harmonic components drawn by nonlinear loads, thereby improving the overall power quality. A control strategy based on instantaneous reactive power theory (p-q theory) is implemented to generate reference currents, which are tracked using a hysteresis current controller to achieve fast dynamic response and accurate compensation. Simulation results demonstrate the effectiveness of the proposed SAPF in reducing Total Harmonic Distortion (THD) of source currents to within IEEE 519 standard limits, while also improving power factor and load balancing. The findings confirm that shunt active filtering provides a flexible and efficient solution for mitigating harmonics in power distribution networks, ensuring stable and reliable operation under varying load conditions.*

**Keywords:** Power Systems, Harmonics, Fault, Shunt Active Filter, Reduction, Distortion

## I. INTRODUCTION

Transformation in the power system has recorded a series of functional theories to increase the electrical power system reliability and efficiency. This transformation have been expanded more as a result of the introduction of new methodologies employing advance communication and control tools, new generation sources, semiconductor technologies and the integration of flexible loading scheme that provide

the regulation of frequency, in the pursuit of energy efficiency .Unfortunately, this technological advancement despite its huge contribution to the electrical power system draw non-sinusoidal current and induce harmonics which also affects the quality of power production and degrades the system's overall power factor.

Non-linear loads and power electronic switching device causes a significant harmonic issue in the power system as a result of extracting harmonic current and reactive power from the power supply source. And because of that they bring about unbalance voltage and neutral current problem in the system network. However, harmonic propagate from one consumer or factory to another causing many objectionable effects on the power system and this harmonic current component do not represent useful active power as a result of the frequency mismatch with the source voltage.

Harmonics are divided into three categories: zero-sequence harmonics, negative-sequence harmonics, and positive-sequence harmonics. Large current magnitudes are present in the harmonic components. While harmonics of the zero sequence flow through the neutral conductor and cause the conductor to overheat, positive-sequence harmonics are components of current harmonics, and negative-sequence harmonics are always found within phase lines and increase the overall system harmonics.

For modern industries with non-linear loads in electrical power systems, power quality issues are a major concern due to the significant time and financial losses.

Harmonic major effects on the power system equipment include: Overheating, Capacitor failure, Vibration, Low power factor, Resonance problem, Communication interference, unwanted circuit breakers or fuses blowing, Overloading and Power

fluctuation. Therefore, to improve the power quality performance, it is obvious that elimination or reduction of harmonics from the power utility system is a must do. The most widely used technique for reducing harmonics is the shunt active power filter (SAPF), which reduces distortion from the harmonic currents by creating a reference current. Shunt active power filters will continue to track the network's reactive power and harmonic current flow while producing reference current from the waveform of distorted current. It should be noted that the shunt active power filter's (SAPF) closed-loop action will assist in real-time reactive power compensation and harmonic reduction with minimal delay.

## II. METHODOLOGY

This work characterized the Oji-River 15MVA (33/11kV) distribution transformer located at Oji-River, Enugu state. The characterization was done to evaluate the performance of the feeder considering the phase characteristics and harmonic content of this Transformer

How it was done

The characterization was done in the control center using a remote supervisory data acquisition and control set up made up of remote terminal unit, programmable logic controller, monitoring

Figure 1: Oji River 132kV Power System in MATLAB

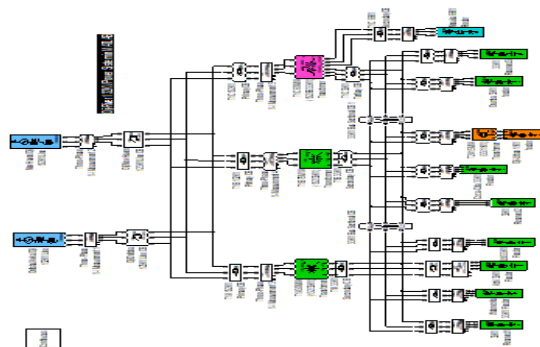


Figure 1: Oji River 11Kv Feeder System in MATLAB

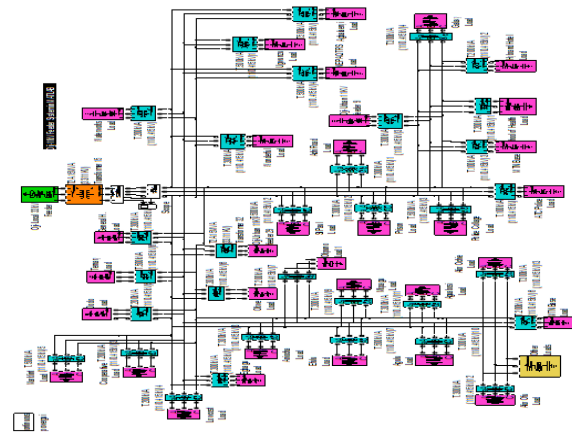


Figure 2: Oji-River 11kv MATLAB/Simulink Feeder System

### A. Method of data collection

The phasor characteristics of the transformer were monitored based on the Power flow analysis load flow model (refer to section 3.5.2) from the set up structure in figure 3.1. The model was used to compute the distribution phase angle, voltage magnitude, real power and apparent power as shown in the table 3.1

Table 1: Orji-River 11kV MATLAB/Simulink Feeder System

BUS NO	15MVA (33/11kV) Transformer	VOLTAGE (p.u)	PHASE ANGLE (Degree)	P LOAD (MW)	Q LOAD (MVar)
1	DH02T22-11F04T400	1.00	0.00	0.14	0.11
2	DH02T22-11F04T427	1.00	0.00	0.27	0.18
3	DH02T22-11F04T474	1.00	0.00	0.18	0.16
4	DH02T22-11F04T401	1.00	0.00	0.08	0.05
5	DH02T22-11F04T477	1.00	0.00	0.11	0.08
6	DH02T22-11F04T463	1.00	0.00	0.06	0.05
7	DH02T22-11F04T460	1.00	0.00	0.10	0.08
8	DH02T22-11F04T457	1.00	0.00	0.14	0.10
9	DH02T22-11F04T407	1.00	0.00	0.05	0.03
10	DH02T22-11F04T479	1.00	0.00	0.14	0.11

BUS NO	15MVA (33/11kV) Transformer	VOLTAGE (p.u)	PHASE ANGLE (Degree)	P LOAD (MW)	Q LOAD (MVar)
11	DH02T22-11F04T466	1.08	0.00	0.13	0.10
12	DH02T22-11F04T467	1.00	0.00	0.17	0.14
13	DH02T22-11F04T464	1.07	0.00	0.18	0.15
14	DH02T22-11F04T432	1.00	0.00	0.00	0.00
15	DH02T22-11F04T416	1.00	0.00	0.01	0.00
16	DH02T22-11F04T403	1.00	0.00	0.05	0.03
17	DH02T22-11F04T470	1.00	0.00	0.05	0.03
18	DH02T22-11F04T469	1.00	0.00	0.05	0.03
19	DH02T22-11F04T418	1.00	0.00	0.05	0.03
20	DH02T22-11F04T484	1.00	0.00	0.14	0.11
21	DH02T22-11F04T473	1.00	0.00	0.27	0.18
22	DH02T22-11F04T454	1.00	0.00	0.18	0.16
23	DH02T22-11F04T475	1.00	0.00	0.08	0.05
24	DH02T22-11F04T412	1.00	0.00	0.11	0.08
25	DH02T22-11F04T455	1.00	0.00	0.06	0.05

Figure 3: Phasor analyzer

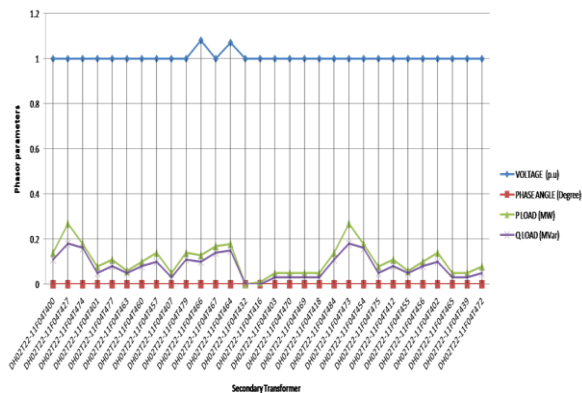
From the result it was observed that Feeder transformer was characterized with nonlinear voltage magnitude. Also the result shows that real and reactive power flow to the load in the secondary distribution transformer can be monitored. To measure the harmonic content in the system, the K-factor technique was used to design a Fourier frequency analyzer. This K-factor technique is designed using the relationship between the root mean square voltages and current of the secondary transformer to compute the voltage harmonic content as shown in the table 2;

Table 2: Result of the current harmonics

Time (s)	Harmonic (%)	Magnitude	RMS voltage	Harmonic order
1	25	254.8	170.9	1
2	47	208.86	154.75	2
3	60	112.83	84.835	3
4	54	65.135	46.245	4
5	16	57.599	40.729	5
6	9.0	50.417	35.650	6
7	7.9	37.612	26.596	7
8	5.0	33.859	23.942	8
9	4.0	30.441	21.772	9
10	3.0	27.635	18.536	10
11	22	25.466	15.341	11
12	1.8	25.83	74.835	12
13	16	22.135	60.200	13
14	1.4	21.599	40.729	14
15	1.2	20.417	35.65	15
16	1.0	18.612	26.596	16
17	12	12.859	23.942	17
18	0.6	10.441	21.772	18
19	0.5	7.635	18.536	19
20	0.0	5.466	15.341	20
Average	14.37			

BUS NO	15MVA (33/11kV) Transformer	VOLTAGE (p.u)	PHASE ANGLE (Degree)	P LOAD (MW)	Q LOAD (MVar)
26	DH02T22-11F04T456	1.00	0.00	0.10	0.08
27	DH02T22-11F04T402	1.00	0.00	0.14	0.10
28	DH02T22-11F04T465	1.00	0.00	0.05	0.03
29	DH02T22-11F04T439	1.00	0.00	0.05	0.03
30	DH02T22-11F04T472	1.00	0.00	0.08	0.05

The Table 1 presents the phasor characteristics of the feeder transformer as it feeds other distribution transformers within the region. The result was determined based on the load flow model and the data obtained was analyzed using load flow Electrical Transient Analyzer Program tool (ETAP tool) as shown in the instrument Figure 3;



The table 2 above presents the characterized results of the feeder from the SCADA network while the harmonic content is analyzed using a Fourier frequency analyzer as shown in figure 3.5. The analyzer measures the total harmonic in the system and analyzes the result at each order using instruments as shown in figure 4.

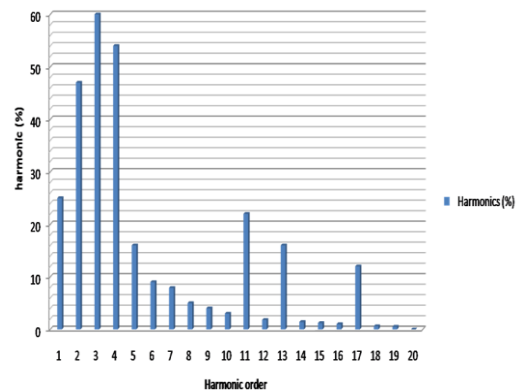


Figure 4: Fourier harmonic analyzer

From figure 4 above, the average total current harmonic in the 11kV feeder system is 14.37%, this result is determined based on the K-factor technique (see equation 3.15) used for harmonic content analysis in electrical power system. This work therefore proposes the use of shunt active harmonic filter to control this harmonic in the case study power system.

### B. System Design

The proposed system will be designed using the following outlined models;

- i. Model of the Oji-River Transformer 15MVA (33/11KV) distribution system
- ii. Harmonic model in the disco system
- iii. Model of the shunt active filter

#### I. Model of the Oji-River Transformer 15MVA (33/11KV) Distribution System

This model designs an equivalent primary distributive system transformer which presents the Oji-River Transformer 15MVA (33/11KV) 11kv feeder system developed using the relationship between the bus and voltage profile identified using figure 5;

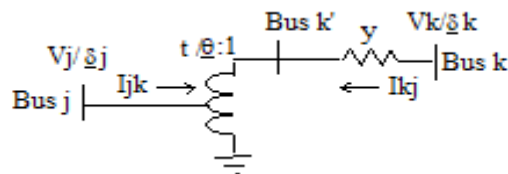


Figure: 5: equivalent distribution transformer

Using the transformer equivalent circuit, the primary and secondary sending (k) and receiving (j) sides are modeled as follows:

$$I_{kj} = \left( V_k \angle \delta_k - \frac{V_j \angle \delta_j}{t \angle \theta} \right) y \quad (1)$$

So for side k,,

$$I_{jk} = -\frac{I_{kj}}{t \angle \theta} \quad (2)$$

For side j,

1.  $I_{kj}$ : Current flowing from node k to node j.
2.  $V_k$ : Voltage magnitude at node k.

3.  $\delta_k$ : Voltage phase angle at node k.
4.  $V_j$ : Voltage magnitude at node j.
5.  $\delta_j$ : Voltage phase angle at node j.
6.  $t$ : Transmission line impedance.
7.  $\theta$ : Angle of transmission line impedance.
8.  $y$ : Admittance of the transmission line.

The power flows that correspond to the power transformer's two ends are

$$S_{jk} = V_{jk} I_{jk}^*, S_{kj} = V_{kj} I_{kj}^* \quad (3)$$

1.  $S$ : Represents complex power, which is a measure of the flow of power in an AC circuit. It includes both real power (P) and reactive power (Q).
2.  $V$ : Represents complex voltage, which is the voltage difference between two points in an AC circuit. It is a complex number with a magnitude and phase angle.
3.  $I$ : Represents complex current, which is the current flowing through a circuit element. It is also a complex number with a magnitude and phase angle.
4.  $^*$ : Denotes the complex conjugate. The complex conjugate of a complex number is obtained by changing the sign of its imaginary part.

#### II Power flow analysis

The power flow program finds the set of unknown parameters that, according to equation 3, result in power balance at every bus. From the standpoint of power flow, each bus has four parameters: active power P, reactive power Q, voltage magnitude V, and voltage angle. The structure below is used to relate these parameters:

$$P_i^{spec} + jQ_i^{spec} = P_i^{calc} + jQ_i^{calc} \quad (4)$$

Where

$$P_i^{calc} + jQ_i^{calc} = V_i I_i^* \quad (5)$$

To put it another way, the power entering the system must match the power specified at each bus. The load flow problem has a size of 2N, where N is the number of buses, because each bus has two unknowns. For each bus, there must obviously be two equations in an effort to resolve the issue. These are from KCL, which has the form for any bus i.

$$P_i^{spec} + jQ_i^{spec} = P_i^{calc} + jQ_i^{calc} = V_i I_i^* = V_i \left[ \sum_{j=1}^N y_{i,j} V_j \right]^* \quad (6)$$

Separating into real and imaginary components yields two equations for bus i,

$$P_i^{spec} = \sum_{j=1}^N |V_i| |y_{i,j}| |V_j| \cos(\delta_i - \delta_j - \theta_{i,j}) \quad (7)$$

$$Q_i^{spec} = \sum_{j=1}^N |V_i| |y_{i,j}| |V_j| \sin(\delta_i - \delta_j - \theta_{i,j}) \quad (8)$$

Where

$$V_i = |V_i| \angle \delta_i, V_j = |V_j| \angle \delta_j, y_{i,j} = |y_{i,j}| \angle \theta_{i,j}$$

### III The Model of Total Harmonic Distortion

The total harmonic voltage distortion is calculated by taking into consideration the system's harmonic order, harmonic current, voltage, and root mean square value.

$$THD_v = [\sqrt{(\sum_{h=2}^{\infty} V_h^2 / V_1)}] \quad (9)$$

$$\text{Or } THD_v = \sqrt{\{(V_{RMS}/V_1)^2 - 1\}}, \quad (10)$$

Where h is the harmonic order,  $V_h$  is the RMS's rated fundamental voltage, and  $V_1$  is the harmonic voltage at harmonic frequency h in RMS. Thus, the fundamental frequency is represented by  $H=1$ .

Similarly, equation (9) is used to find the system's total harmonic current, and equation (11) is used to replace voltage with current.

$$THD_i = \left[ \sqrt{\frac{\sum_{h=2}^{\infty} I_h^2}{I_1}} \right] \quad (11)$$

$$\text{or } THD_i = \sqrt{\left\{ \left[ \frac{I_{RMS}}{I_1} \right]^2 - 1 \right\}} \quad (12)$$

The RMS voltage and current can now be expressed in terms of THD since equations 10 and 12 are used to determine the current system's total current and voltage harmonics, where  $I_h$  is the harmonic frequency  $h_f$  at which the harmonic current occurs in RMS and  $I_1$  is the rated fundamental current in RMS.

$$V_{RMS} = \sqrt{\sum_{h=1}^{\infty} V_h^2} \quad (13)$$

$$I_{RMS} = \sqrt{\sum_{h=1}^{\infty} I_h^2} \quad (14)$$

### IV Model of the K-Factor Technique

This method functions at harmonic frequencies with reduced losses and is especially made for nonlinear loads;

Equation 15 below illustrates the model, which is the ratio of eddy current losses when supplying nonlinear loads and linear loads;

$$K = \frac{P_i}{P_f} = \sum_{h=1}^{h=h_{\max}} I_h^2 h^2 \quad (15)$$

Where;

K is the k factor

Pi is the eddy current losses on linear load

Pf is the eddy current loss on nonlinear load

H is the harmonics value

$h_h$  Is the harmonic current (p.u)

### C. Mathematical Model of SAPF

The three-phase power source with filter connected in parallel to the distribution load (nonlinear load) can be used to model the SAPF. Figure 7 illustrates the basic

design of a shunt active power filter coupled to a three-phase, three-wire system.

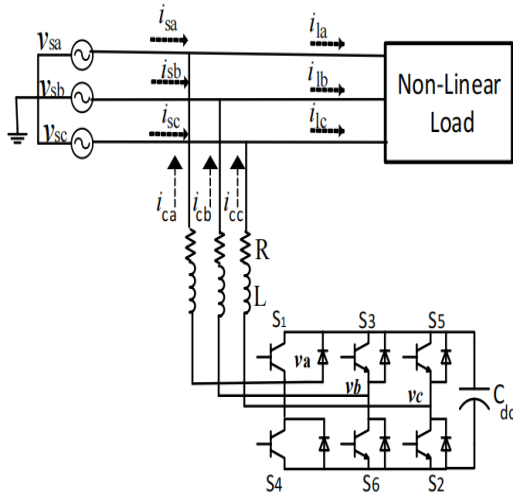


Fig. 6: Fundamental Structure of SAPF

Where;  $V_{sa}$ ,  $V_{sb}$  and  $V_{sc}$  represent source voltages

$i_{la}$ ,  $i_{lb}$  and  $i_{lc}$  represent load currents

$i_{ca}$ ,  $i_{cb}$  and  $i_{cc}$  represent the compensating currents injected

$$\begin{cases} L \frac{d}{dt} i_{ca} = v_{sa} - R i_{ca} - v_a \\ L \frac{d}{dt} i_{cb} = v_{sb} - R i_{cb} - v_b \\ L \frac{d}{dt} i_{cc} = v_{sc} - R i_{cc} - v_c \\ C_{dc} \frac{d}{dt} v_{dc} = f_a i_{ca} + f_b i_{cb} + f_c i_{cc} \end{cases}$$

Where;  $f_a$ ,  $f_b$ , and  $f_c$  are switching functions. Inductance and resistance of the filter are denoted by  $L$  and  $R$  respectively.  $C_{dc}$  is the capacitance at the DC link. This matrix can also be written as

$$\frac{d}{dt} \begin{bmatrix} i_{ca} \\ i_{cb} \\ i_{cc} \\ v_{dc} \end{bmatrix} = \begin{bmatrix} -\frac{R}{L} & 0 & 0 & 0 \\ 0 & -\frac{R}{L} & 0 & 0 \\ 0 & 0 & -\frac{R}{L} & 0 \\ \frac{f_a}{C_{dc}} & \frac{f_b}{C_{dc}} & \frac{f_c}{C_{dc}} & 0 \end{bmatrix} \begin{bmatrix} i_{ca} \\ i_{cb} \\ i_{cc} \\ v_{dc} \end{bmatrix} + \frac{1}{L} \begin{bmatrix} v_{sa} - v_a \\ v_{sb} - v_b \\ v_{sc} - v_c \\ 0 \end{bmatrix}$$

The transformation matrix required for conversion from abc to an arbitrary rotating dq0 reference frame is given as

$$T = \frac{2}{3} \begin{bmatrix} \cos\theta & \cos(\theta - \frac{2\pi}{3}) & \cos(\theta + \frac{2\pi}{3}) \\ \sin\theta & \sin(\theta - \frac{2\pi}{3}) & \sin(\theta + \frac{2\pi}{3}) \\ \frac{1}{2} & \frac{1}{2} & \frac{1}{2} \end{bmatrix}$$

Therefore, the addition of three-phase voltages and currents results in zero as shown as

$$\begin{aligned} i_{sa} + i_{sb} + i_{sc} &= 0 \\ v_{sa} + v_{sb} + v_{sc} &= 0 \end{aligned}$$

Eq. 3 represents the currents in dq frame

$$\frac{d}{dt} \begin{bmatrix} i_{cd} \\ i_{cq} \\ v_{dc} \end{bmatrix} = \begin{bmatrix} -\frac{R}{L} & \omega & -\frac{f_d}{L} \\ -\omega & -\frac{R}{L} & -\frac{f_q}{L} \\ \frac{f_d}{C_{dc}} & \frac{f_q}{C_{dc}} & 0 \end{bmatrix} \begin{bmatrix} i_{cd} \\ i_{cq} \\ v_{dc} \end{bmatrix} + \frac{1}{L} \begin{bmatrix} v_d \\ v_q \\ 0 \end{bmatrix}$$

Where the switching state functions of the system in dq reference frame are denoted by  $f_d$  and  $f_q$  and  $\omega$  is the supply angular frequency. Eq. 3 can be re-written to get Eq. (3)

$$\begin{cases} L \frac{d}{dt} i_{cd} = v_d - R i_{cd} + \omega L i_{cq} - f_d v_{dc} \\ L \frac{d}{dt} i_{cq} = v_q - R i_{cq} - \omega L i_{cd} - f_q v_{dc} \\ C_{dc} \frac{d}{dt} v_{dc} = f_d i_{cd} + f_q i_{cq} \end{cases}$$

## V. Shunt Resistance Power

The RMS equations 11 and 12 are used to define the model in equation 13, which calculates the real (or active) power dissipated in a shunt resistor by taking into account the total harmonic current and voltage related.

$$Q_l = \frac{1}{2} \sum_{h=1} V_h I_h = \frac{1}{2} \sum_{h=1} I_h^2 R_h = \frac{1}{2} \sum_{h=1} (V_h^2 / R_h) \quad (16)$$

Where  $R_h$  is the resistance at the hth harmonic

## VI. Shunt Inductance Power

Pure Inductance power is determined as;

$$Q_l = \frac{1}{2} \sum_{h=1} V_h I_h = \frac{1}{2} \sum_{h=1} I_{h(RMS)}^2 R_{h(RMS)} \quad (17)$$

Where  $V_1 = j2\pi f_1 L I_1$

$$V_h = j2\pi f_H L I_H$$

$f_1$  = fundamental frequency

Thus

$$V_h/V = h \times \frac{I_h}{I_1} \quad (18)$$

$$Q_{L(pu)} = \sum_{h=1} h \times I_{h(pu)}^2 = \sum_{h=1} (V_{h(pu)}^2 / h) \quad (19)$$

## VII. Power in Shunt Capacitance

Power in pure capacitance is determined as;

$$Q_c = -\frac{1}{2} \sum_{h=1} V_h I_h = -\sum_{h=1} V_{h(RMS)} I_{h(RMS)} \quad (20)$$

A negative sign here means that the load is receiving reactive power

And

$$V_1 = \frac{I_1}{j2\pi f_1 C} \quad (21)$$

$$V_{h1} = \frac{I_1}{j2\pi h f_1 C} \quad (22)$$

$$\frac{V_1}{V_h} = \frac{I_h}{h I_1} \quad (23)$$

$$Q_{C(pu)} = \sum_{h=1} h \times V_{h(pu)}^2 = \sum_{h=1} (I_{h(pu)}^2 / h) \quad (24)$$

Equations 23, 15, and 18 are now combined to create the matching Shunt RLC models (Y), with the frequency-dependent S-parameters of the shunt RLC network shown in figure 6. At each frequency in the

vector of modeling frequencies, the block first determines the ABCD-parameters for the given resistance, inductance, and capacitance. Then, it uses the Radio Frequency Toolbox to convert the ABCD-parameters to S-parameters. In this circuit,  $D = 1$ ,  $C = Y$ ,  $B = 0$ , and  $A = 1$ .

Where:

$$Y = \frac{-LC\omega^2 + j\left(\frac{L}{R}\right)\omega + 1}{jL\omega}; \quad \omega = 2\pi f. \quad (25)$$

The shunt RLC object is a two-port network as shown in Figure 7

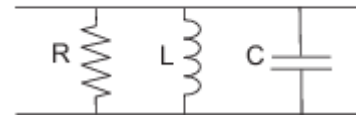


Figure 7: shunt RLC model

## D. Implementation of the Model

The application of the mathematical transfer functions of parameters related to the power system that were established by the different models in the work's earlier section is covered in this section. Simulink, mathematical models, the power system toolbox, and the optimization toolbox will be used to implement the model, as shown in Figures 9, 10, 11, and 12.

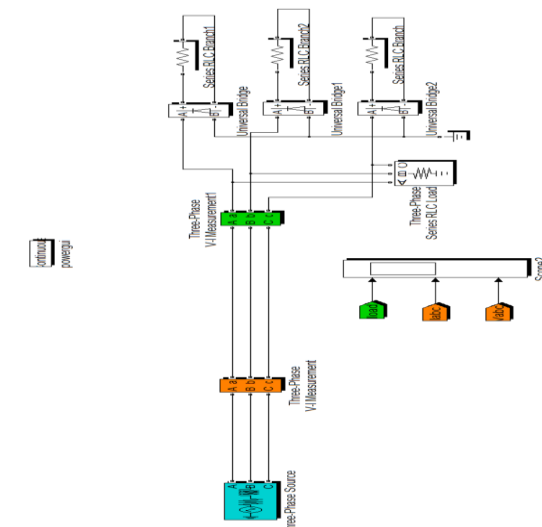


Figure 9: The model of the three phase system with a resistive load.

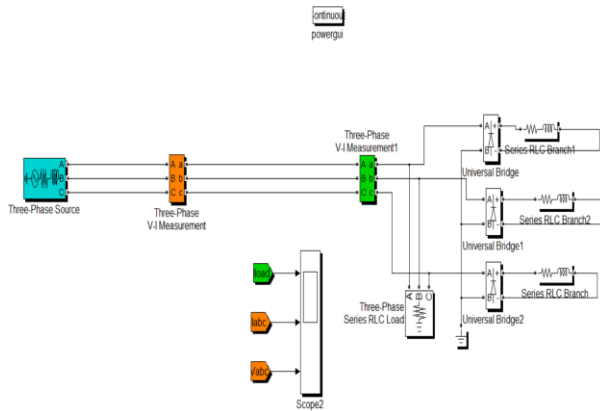


Figure 10: The model of the three phase system with a nonlinear load.

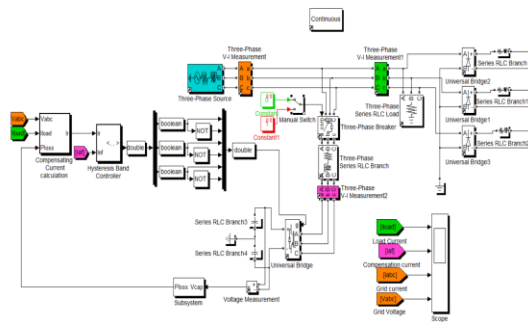


Figure 11: The model of the three phase system with a nonlinear load and shunt active power filter in open position

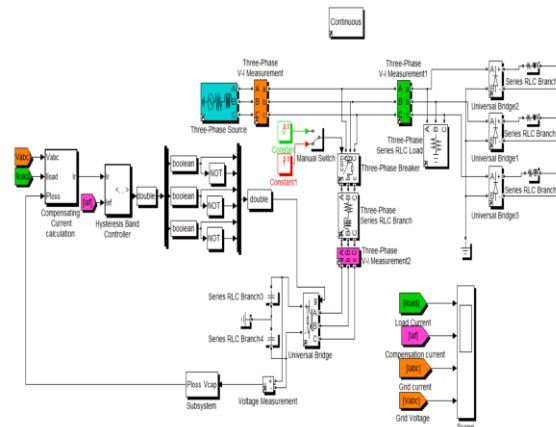


Figure 12: The model of the three phase system with a nonlinear load and shunt active power filter in close position.

### The three-phase system model featuring a shunt active harmonic filter

Active power filter is a bidirectional converter. It operate as rectifier to charge the capacitors in one direction and operate as an inverter to generate a required opposite harmonics for system.

From the implemented model presented in figure 11 and 12, the Oji-River Transformer 15MVA (33/11kV) distributive system redesigned with shunt active harmonic filter as shown in equation 3.24; the 11kV distributive system was developed using the model in the equation 3.1 and the total harmonic was measured using the model in equation 11 and 12 or current and voltage harmonics respectively.

The Shunt Active Power Filter is connected in shunt with the load the aim is to suppress the harmonics by injecting a compensating current to the system. A reference value is established and compared to the actual capacitor voltage. In figure 11 and 12, three-phase ac voltage source is connected to the three-phase voltage and current measurement block. The source currents are measured and output is shown in data acquisition scope as a grid voltage and current. On the other side non-linear load is connected to the three-phase voltage and current measurement block. The output current and voltage of non-linear load is seen in scope as a load current ( $I_{load}$ ). APF is connected to the wires of source currents and the current of APF is measured in scope as active filter current ( $I_{af}$ ).

### III. RESULTS AND DISCUSSION

This chapter will discuss the results of the simulation models implemented using the parameters in table 4; the results will present the performance of the improved Oji-River Transformer 15MVA (33/11kV) 11kV feeder system with shunt active harmonic filter.

Table 3: Simulation parameters

Parameters	Values
Oji-River feeder rating	15MVA
Transformer type	Three phase power transformer
Load capacity	15MVA (33KV/11kV)
Inductance	0.05H
Total reactive power	600Mvar
Frequency	50Hz
Maximum frequency	2500Hz
Start time	0.1s
Base value	1.0
Signal number	1,2 or 3
Frequency axis	Harmonic order or Hertz
Window style	FFT window or signal

### A. Results

The performance of the feeder system is examined in this section using the simulation parameters in table 4.1; the results were obtained by simulating the models used in figure 12 and are displayed alongside the voltage performance in figure 3 below;

The Sim-power system Toolbox was used to obtain the simulation results in the MATLAB/Simulink environment. Here, the analysis is displayed during the Active Power Filter's ON and OFF times using a breaker.

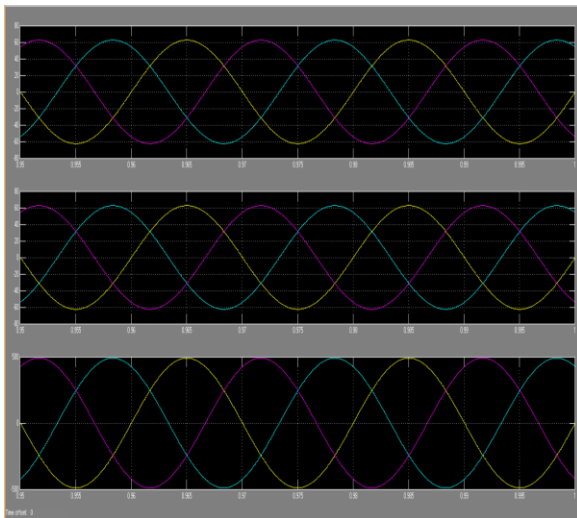


Figure 13 Current and Voltage waveform of a three-phase resistive load system. The current and voltage

are in phase, their waveforms are sinusoidal and negligible harmonics observed.

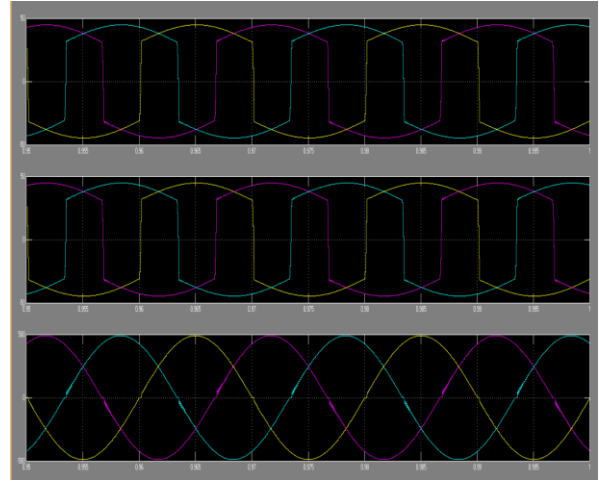


Figure 14: Current and Voltage waveform of a three phase nonlinear or inductive load system.

The current and voltage are out of phase and the current sine wave is not sinusoidal.

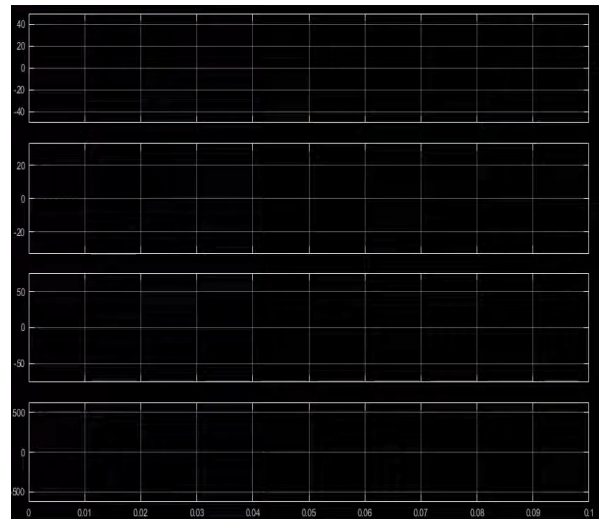


Figure 15: the scope result before simulation

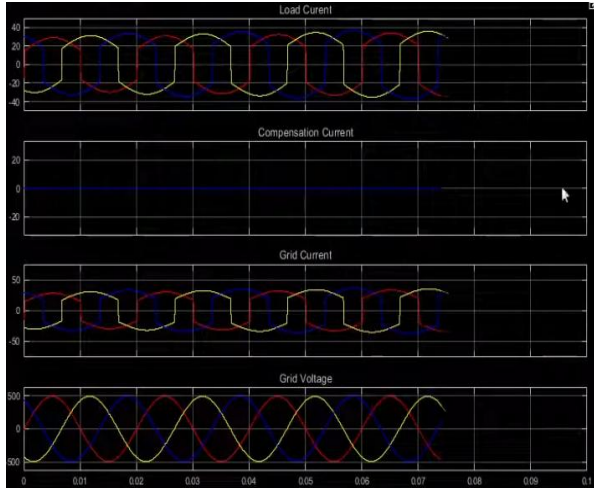


Figure 16: the simulation results with shunt active power filter in open position

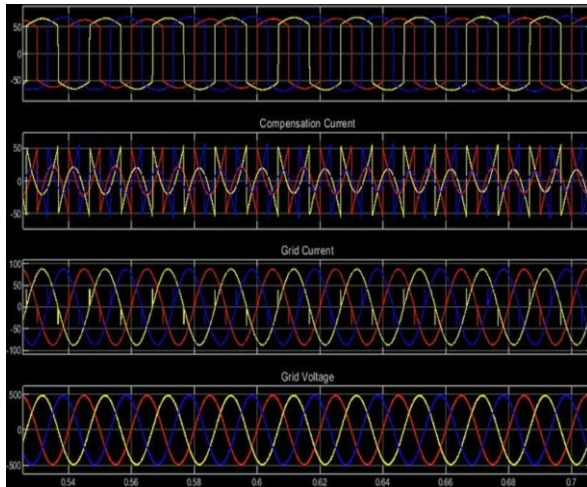


Figure 17: the simulation results with shunt active power filter in close position

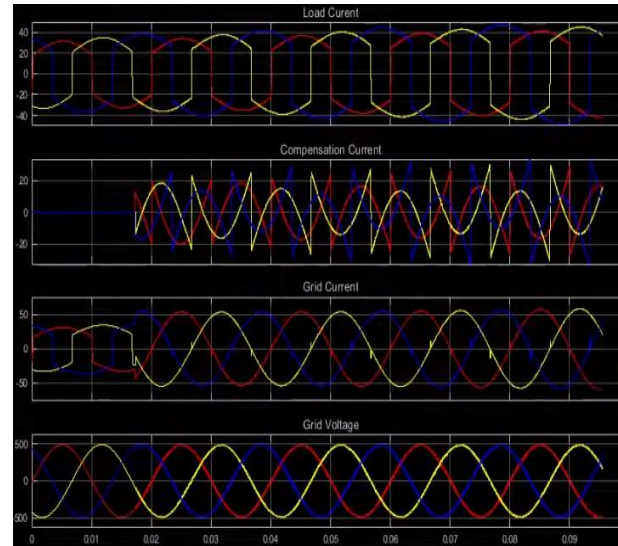


Figure 18: the simulation results with shunt active power filter in close and opening position.

### B. FFT Analysis

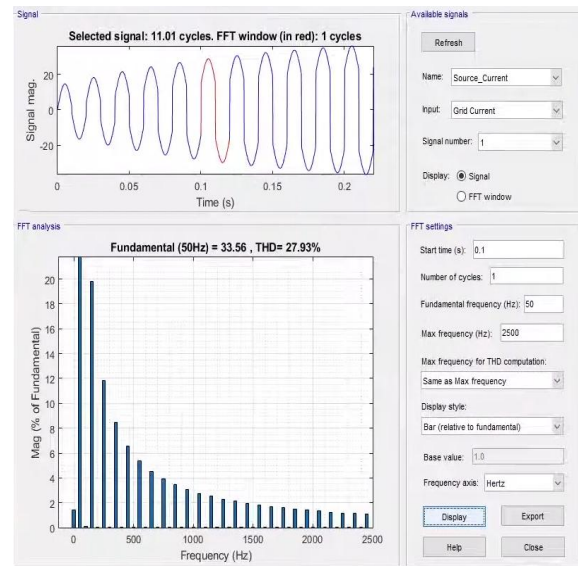


Figure 19 Fast Fourier Transformation analysis of source current without SAPF

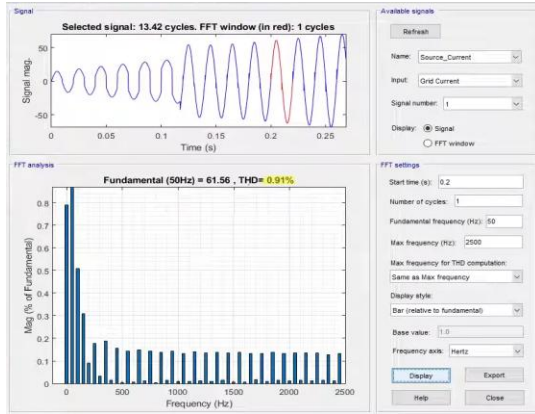


Figure 20: Fast Fourier Transformation analysis of source current SAPF

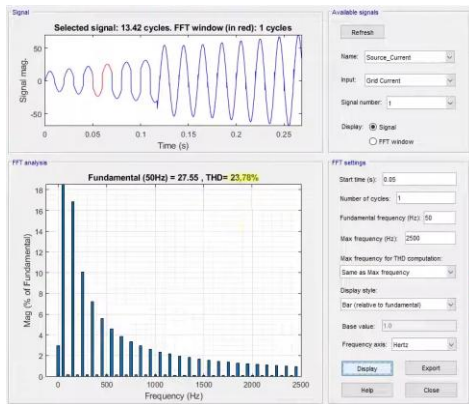


Figure 21: Fast Fourier Transformation analysis of source current immediately SAPF circuit is closed.

### C. Comparative Analysis

The comparative analysis of the above design is the Total Harmonic Distortion (THD) of

Figure 22: Fast Fourier Transformation

analysis of load current the system is displayed using the FFT-based current control method between the system with and without SAPF to 27.93% and with SAPF, it goes down to 0.91%.

Also comparative analysis has been performed to compare and contrast the performance of the feeder before and after connection with the proposed and designed shunt active harmonic filter. The result is presented as shown in table 4;

Figure 22 Fast Fourier Transformation analysis of load current

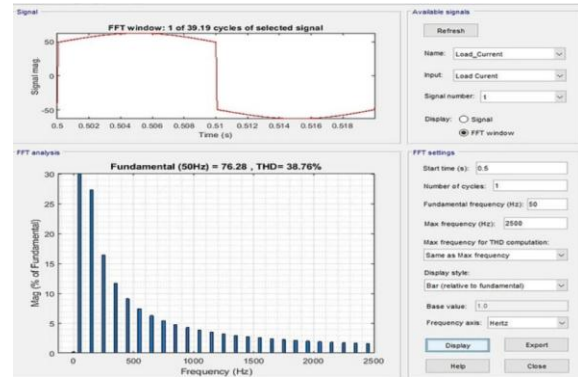


Table 4: Comparative result

Harmonic order	H(%) without filter	H(%) with filter
1	25	0.50
2	47	0.08
3	60	0.06
4	54	0.08
5	16	0.05
6	9.0	0.08
7	7.9	0.04
8	5.0	0.05
9	4.0	0.08
10	3.0	0.04
11	2.2	0.33
12	1.8	0.06
13	1.6	0.17
14	1.4	0.03
15	1.2	0.03
16	1.0	0.01
17	1.2	0.01
18	0.6	0.00
19	0.5	0.00
20	0.0	0.00
THD %	14.37	0.085

From the table 4, the results of the feeder with SAPF and without SAPF have been analyzed and presented with respect to current harmonic. From this data presented, it was observed that the average harmonic in the new system was only 0.085% compared to the feeder without filter at 14.37%. This result is analyzed using the frequency analyzer as shown in figure 23;

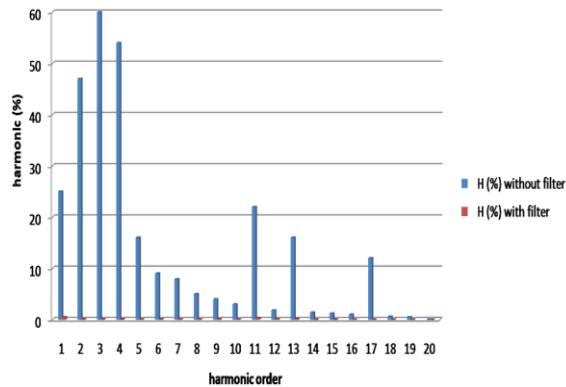


Figure 23: Comparative Bar analysis between System without and with SAPF

From this comparative response obtained in the analyzer in figure 23, it is obvious that the harmonic have been reduced to the lowest value as shown. This is the reason the bar representing the H(%) with filter is very small in bar size compared to the H(%) without filter.

Harmonic in power distributive system equipment's are nonlinear signal induced from load or power electronics controlled devices used to optimize or stabilize the power flow analysis in a distribution system. Overtime, the need to reduce this harmonic have been researched upon, various technique proposed and even implemented. However, today in the conventional power system like the characterized Oji River 11KV feeder, it was observed that shunt active power filters (SAPF) with current controlled voltage source inverter (CCVSI) is used effectively to mitigate the harmonics and to balance the phases sinusoidal source currents by generating and injecting current to compensate the harmonic currents cause by nonlinear loads. From the characterized result, it was observed that the feeder system has 14.37% of voltage harmonic. This work has been modeled and simulates a filter using shunt RLC elements to mitigate the voltage harmonic effect on the system to 0.085%.

By reducing the current harmonic response to 0.085%, this work has effectively enhanced the Oji River 11KV feeder transformer's performance. A shunt active harmonic filter was designed in order to achieve this. This was done using shunt active power filters (SAPF) with current controlled voltage source inverter (CCVSI). The filter develop was connected to the case study feeder transformer and simulated using simulink

available in MATLAB and other desired toolbox. The result shows that the current harmonic was removed to the lowest level. According to simulation results, an active shunt power filter improved the quality of power in the power system by removing reactive current and harmonics from the source current, bringing it into sinusoidal phase with the source voltage.

## REFERENCES

- [1] Panda, G., Dash, S. K., Ray, P. K., & Puan, P. S. (2013). *Performance Improvement of Hysteresis Current Controller Based Three-Phase Shunt Active Power Filter for Harmonics Elimination in a Distribution System*. In *Advances in Computing, Communication, and Control*, ICAC3 2013. Springer. SpringerLink
- [2] Imam, A. A., Sreerama Kumar, R., & Al-Turki, Y. A. (2020). *Modeling and Simulation of a PI Controlled Shunt Active Power Filter for Power Quality Enhancement Based on P-Q Theory*. *Electronics*, 9(4), 637. MDPI
- [3] Szromba, Andrzej. (2024). *Improvement of the Source Current Quality for a Shunt Active Power Filter Operating Using Hysteresis Technique with Stabilized Switching Frequency*. *Energies*, 17(20), Article 5098. MDPI
- [4] Suhendar; Teguh Firmansyah; Alief Maulana; Zuldiag; Vektor Dewanto. (2017). *Shunt Active Power Filter Based on P-Q Theory with Multilevel Inverters for Harmonic Current Compensation*. Simulink MATLAB. Zenodo
- [5] R. Balamurugan & R. Nithya. (2015). *Photovoltaic Based Shunt Active Power Filter Using P-Q Theory for Enhancing the Power Quality*. *Electrica*, 15(2), 1959-1964. electricajournal.org
- [6] Miss. Dhanshri Sarjerao Pawar, Dr. K. Vadirajacharya. (2016). *Design of Shunt Active Filter to Improve Power Quality using P-Q Theory*. *IJERT*, 5(3), March 2016. *IJERT*
- [7] Krishna Veer Singh; Ravinder Kumar; Hari Om Bansal; Dheerendra Singh. (2020). *Hardware Realization of a Single-Phase-Modified P-Q Theory-Based Shunt Active Power Filter for Harmonic Compensation*. In *Intelligent*

Communication, Control and Devices. Springer.  
SpringerLink

- [8] Tilak Giri; Ram Prasad Pandey; Sabin Bhandari; Sujan Moktan; Lagat Karki. (Year). *Design and Simulation of Three Phase Three Wire Shunt Active Filter using Instantaneous PQ Theory*. Journal of the Institute of Engineering (Nepal). Nepjol
- [9] Kamel, K., Laid, Z., Abdallah, K., & Anissa, K. (2019). *Performance of Shunt Active Power Filter Using STF with PQ Strategy in Comparison with SOGI Based SRF Strategy Under Distorted Grid Voltage Conditions*. In Renewable Energy for Smart and Sustainable Cities, ICAIRES 2018. SpringerLink
- [10] Imad Aboudrar; Soumia El Hani; Hamza Mediouni; Ahmed Aghmadi. (2019). *Active Disturbance Rejection Control of Shunt Active Power Filter Based on P-Q Theory*. In Recent Advances in Electrical and Information Technologies for Sustainable Development. Springer.